

# Relationship between the focal mechanism of magnitude $M_L$ 3.3 seismic event induced by mining and distribution of peak ground velocity

Józef Dubiński<sup>1</sup>, Krystyna Stec<sup>1\*</sup> and Grzegorz Mutke<sup>1</sup>

<sup>1</sup>Central Mining Institute, 40-166 Katowice, Poland

**Abstract.** The relationship between seismic radiation pattern generated by a strong mining induced seismic event and the distribution of peak ground velocity in the epicenter area has been presented. It was a seismic event with the local magnitude  $M_L = 3.3$  occurred on June 21, 2016 in the Upper Silesian Coal Basin (USCB) in Marcel Mine. Calculated values of the peak ground velocity, taking into account the amplification coefficient, were the basis for the development of the  $PGV_H^{amp}$  map. The resulting distribution of  $PGV_H^{amp}$  isolines and the measured velocity amplitudes point to significant differences. That fact indicates that some additional factors can impact on the seismic effect observed on the surface. One of them could be a focal mechanism of seismic event. Focal mechanism of the  $M=3.3$  induced seismic tremor, were calculated by the moment tensor inversion method. The tremor was characterized by a normal slip mechanism with 87% shear component. Comparison of seismic pattern for  $S$ -wave at individual stations allowed confirms a relation between directionality of the seismic radiation pattern for  $S$ -wave and the recorded peak ground velocities and explain the observed anomaly.

## 1 Introduction

Determining the intensity of earthquakes and of seismic events induced by mining on the surface is an extremely complex issue since the magnitude of the seismic effect on the surface is determined by many factors, including: seismic energy or seismic magnitude of a tremor, epicentral distance, geological structure of the rock mass on the path of seismic waves, seismogeological parameters of the near surface as well as many others [1, 2, 3, 4, 5, 6]. Therefore, it is difficult to estimate seismic intensity (peak ground velocity,  $PGV$  and acceleration,  $PGA$ ) only as a function of such seismic parameters as seismic energy and epicentral distance. In addition, although one of the most important reasons for the observed local intensity of mining tremors is the amplification of ground motion by the subsurface soil layers, the inclusion of this phenomenon does not completely resolve the observed variability in the distribution of the above-described parameters of mining tremors. Therefore, studies have been undertaken to clarify the large local discrepancies between measured values and prognostic data based on empirical formulas for Upper

---

\*Corresponding author: [kstec@gig.eu](mailto:kstec@gig.eu)

Silesia Coal Basin (USCB) [1]. The solutions obtained in this field are not only cognitive but also practical because, due to the high seismicity induced by mining activity, a more precise characteristic of seismic effects on the surface is an extremely significant issue. It is an important element of both the protection of the environment and the formation of a partnership between mining enterprises and local communities, particularly in terms of the acceptance of mining activities. USCB is one of the high seismic areas in Poland induced by mining activity [7, 8, 9, 10, 11, 12]. In the years 2006-2016 there were 13216 shocks with magnitude above 1.6, including 31 very strong ( $M_L$  magnitude =  $3.26 \div 4.11$ ) comparable to weak earthquakes. In addition, USCB is a heavily urbanized area, causing seismic impacts, particularly in the case of high-energy tremors, which is a major problem not only in technical but also in social area. For this reason, research into the improvement of research methods and state of the art has been carried out for many years.

## 2 Ground motions parameters of strong mining induced seismic event of magnitude $M_L = 3.3$ recorded on June 21, 2016

Two different values of the peak ground velocity  $PGV_{Hp}$  and acceleration  $PGA_{Hp10}$  were recorded by seismic surface stations in the epicentral distance for the tremor of magnitude  $M_L = 3.3$ . The values of the horizontal parameters  $PGV_{Hp}$  and  $PGA_{Hp10}$  are summarized in Table 1.

**Table 1.** The ground motions parameters of strong mining induced seismic event of magnitude  $M_L = 3.3$  recorded on June 21, 2016.

Station	$PGV_{Hp}$ , m/s	$PGA_{Hp10}$ , $m/s^2$ (frequency band up to 10 Hz)	Epicentral distance, m
S1	0.0159	0.535	722
S2	0.0304	1.095	761
S3	0.0555	1.711	115
S4	0.0205	0.542	1100
S5	0.0015	0.035	4,500
S6	0.0012	0.025	5,193

The maximum values of velocity and acceleration on the recorded seismograms were related to the direct transverse waves SP and SH. Figure 1 shows the vibration velocity seismograms on station S2, located in the 761 m from epicentre. Several decades of monitoring of seismic events in the Upper Silesia prove that the highest amplitudes of PGV and PGA from mining seismic events are recorded in the epicenter zone and are derived from transverse waves. For these mining induced seismic event the short duration of the main phase of the vibration is also characteristic (Figure 1). The maximum values of  $PGV_{Hp}$  and  $PGA_{Hp10}$  were recorded at S3 station at a distance of 115 m. This station was located in a epicentral zone, which explains very high registered values. At the next two stations S1 and S2 located at the distance of 722 and 761m, the velocity amplitudes were smaller but their values differences were two times each other. The subject of research is therefore to determine the cause of this discrepancy, which is not a factor of seismic energy or epicentral distance.

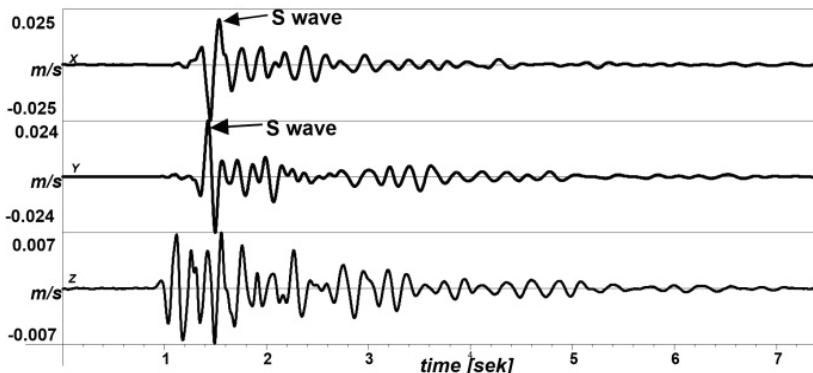


**Fig. 1.** Velocity ground motion recorded on station S2 in epicentral zone from the mining induced seismic event of magnitude  $M_L = 3.3$  on June 21, 2016.

One of the factors influencing the value of ground motions parameters is the geological structure of the near surface quaternary layers, usually characterized by low velocity propagation of seismic transverse wave in Upper Silesia geological condition. The parameter that expresses the influence of quaternary overburden layers on vibration intensity is the  $W_f$  amplification factor, which varies in a given location depending on the frequency range and the seismogeological parameters of the overlay layers [1, 3, 7, 13]. In Marcel mine, there is a locally variable quaternary layer (several to tens of meters), characterized by low velocities of seismic waves propagation. Amplification factor  $W_f$  was determined based on recognition of lithological of quaternary and tertiary structures and their thickness. In the area of the location of seismic stations there the tremor on June 21, 2016 was recorded, the amplification factor varies from 1.3 to 2.0 (Figure 2). This does not explain, however, the large discrepancies in the values of recorded ground motions parameters at stations S1 and S2.

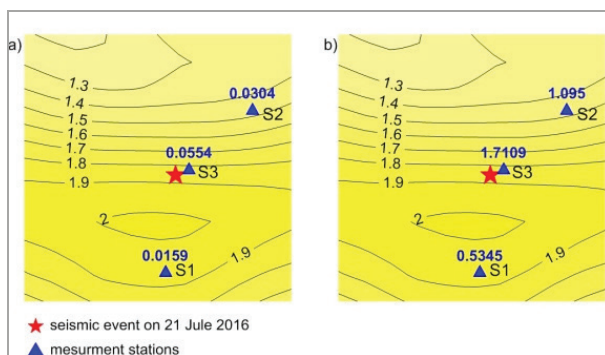


**Fig. 2.** Distribution of  $W_f$  amplification factor and measured values of  $PGV_{Hp}$ , m/s (a) and  $PGA_{Hp10}$ ,  $m/s^2$  (b) for the tremor of  $M_L = 3.3$  on June 21, 2016.

### 3 Distribution of peak ground velocity $PGV_{Hmax}$ for the tremor on June 21, 2016

The assessment of the ground motions intensities generated by induced mining tremors is so far limited to the parameter of amplitude of horizontal vibration velocity  $PGV_H$  and time

duration. The Mining Seismic Instrumental Intensity Scale MSIIS-15 used in coal mines to study impact effect in buildings are based on these two parameters [12, 14]. In this article we used the method of determining the distribution of  $PGV_H$  parameter consists of two basic stages [1].

Determination of the amplitude of horizontal vibration velocity  $V_{MD}$  for bedrock foundation in USCB as a function of seismic energy and epicentral distance, for seismic energy  $E$  in the range  $2 \cdot 10^5 \div 5 \cdot 10^8$  J (magnitude  $M_L$  in the range  $1.8 \div 3.6$ ; the energy of the tremors in Polish mines is converted into the local magnitude according to the formula:  $M = (\log E - 1.8) / 1.9$ ):

$$V_{MD} = [1.48 \cdot 10^{-3} (\log E)^{1.23} - 0.011] \cdot [1.55R^{0.135} \exp(-0.77R) + 0.040] \quad (1)$$

where:  $E$  – tremor seismic energy, J,

$V_{MD}$  – maximum horizontal vibration velocity amplitudes of bedrock, m/s,

$R^2 = D^2 + h^2$ ,  $D$  – epicentral distance, km;  $h$  – depth of source, km.

Calculation of the horizontal vibration velocity  $PGV_H^{amp}$  as the multiplication of  $V_{MD}$  by the amplification factor  $W_f$ :

$$PGV_H^{amp} = V_{MD} \cdot W_f \quad (2)$$

where:  $W_f$  – amplification factor for S waves dimensionless [15].

The distribution of velocity isolines according to relation 2 for the analysing seismic event of magnitude  $M=3.3$  is shown in Fig. 3a. As the measured values at individual seismic stations in the epicentral zone deviated from the values determined in accordance with formula 2, the new calculation of the peak ground velocity distribution considers the velocity  $PGV_{Hp}$  measured on the surface seismic stations were made. The methodological approach allows for the inclusion of empirical PGV values recorded on six seismic stations. The calculation procedure was as follows [15].

- For each seismic station, an area with a radius  $r = 250$  m is determined, within which the  $PGV_{Hp}(S_i, 0)$  value recorded by the seismic devices is assumed.
- In nodal points located at a distance of  $r > 250$  m from these stations, the value of corrected amplitude  $PGV_H^{kor}(r_i)$  of the horizontal velocity is approximated by the formula:

$$PGV_H^{kor}(r)_i = d \cdot PGV_{Hp}(S_i, 0) + (1-d) \cdot PGV_H^{amp} \quad (3)$$

where:  $PGV_{Hp}(S_i, 0)$  – the value of the peak horizontal vibration velocity measured at the nearest  $S_i$  seismic station from a given node, located at  $r_i$  from the node,  $PGV_H^{amp}$  – value calculated from relationship 2 in the node located at distance of  $r_i$  from  $S_i$  seismic station  $d = 250 / r_i$  for  $r_i > 250$ m;  $d = 1$  for  $r_i \leq 250$ m.

The results of the  $PGV_H^{kor}(r_i)$  include the amplitude values recorded at the all seismic stations. The results of the calculations of the corrected peak ground velocity  $PGV_H^{kor}(r_i)$  are shown in Figure 3b. When analysing this distribution, it is important to note that the distribution of velocity isolines as compared to Figure 3a, as well as the measurements values of the velocity by particular seismic stations are distinctly more compatible. It can be stated that the obtained map of the corrected distribution of the horizontal component amplitude of vibration velocity  $PGV_H^{kor}(r_i)$  significantly better reflects real state and allows for a more reliable assessment of vibration intensity and its impact on building objects using existing instrumental scales MSIIS-15, which is based on the vibration velocity [12, 14].

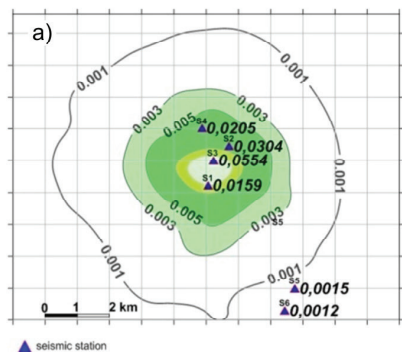


**Fig. 3a.** Distribution of the velocity amplitudes  $PGV_H^{amp}$  calculated according to formula 2 for the mining induced seismic event of magnitude  $M_L = 3.3$ .

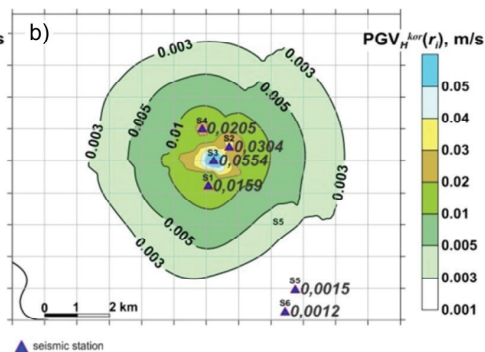


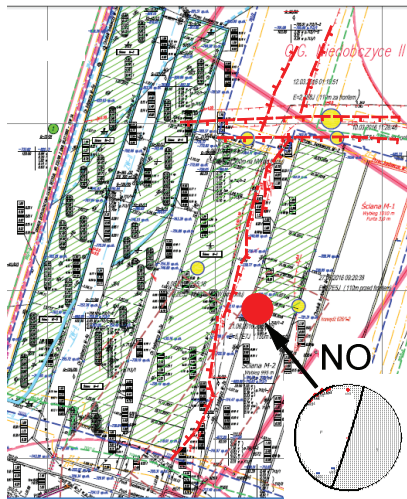
**Fig. 3b.** Distribution amplitude of the corrected velocity  $PGV_H^{kor}(r_i)$  for the mining induced seismic event of magnitude  $M_L = 3.3$ .

## 4 Focal mechanism of $M_L = 3.3$ strong mining induced seismic event recorded on June 21, 2016

Excluding the influence of, epicentral distances and amplification factor, it was assumed that the radiations pattern for waves, which depends on the focal mechanism, can be a cause of the discrepancy on  $PGV_{Hp}$  and  $PGA_{Hp10}$  recorded at measurement station S1 and station S2. The focal mechanism was calculated using the seismic moment tensor inversion method (SMT) in the time domain from amplitudes and polarity of  $P$ -wave with FOCI software [16]. The SMT analysis was based on the seismograms recorded by underground seismic network of Marcel mine. The 16 stations are horizontally and vertically spaced from the seismic events at distances ranging from 0,5 to 4 km and from 0,1 to 0,8 km, respectively. The stations surrounding the area of the longwall, which was the basis for the correct determination of tremor focus localisation and its mechanism. Angular parameters of the focal mechanism are calculated with error 15°. Figure 4 shows the parameters of the focal mechanism. The full, deviatoric, and pure shear moment tensor was calculated using the L2 norm as a measure of the misfit. This tremor was characterized by a normal slip mechanism with 87% share of the shear component. The remaining explosive component and uniaxial compression were 12 and 1% respectively. As the rupture plane, an azimuth plane was selected located almost at the NE –SW (strike 28°) and a dip of 88° facing to the east. The azimuth of the selected nodal plane could be correlated with the azimuth of the fault zone in this region (Fig. 4).

## 5 Seismic wave radiation pattern for S-wave

Seismic waves radiation pattern in the rock mass depends on the rupture process in the tremor's source. Based on recorded seismograms of tremors, the displacement field in different directions and at different distances from the source area can be determined. A theoretical description of the seismic radiation pattern can be found in Aki [17].



Focal mechanism parameters*				
Nodal plane A,B $\Phi A/\delta A/\lambda A$ $\Phi B/\delta B/\lambda BA$	Axis P,T $\Phi P/\delta P$ $\Phi T/\delta T$	component TMS, %		
		ISO	CLVD	DBCP
28/88/-89 166/3/- 122	289/47 106/43	12	1	87

\*  $\Phi A, B$  – strike A,B;  $\delta A, B$  – dip A,B;  
 $\lambda$  – slip angle;  $\Phi P, T$  – strike P,T;  
 $\delta P, T$  – plunge P,T; ISO – explosion; CLVD –  
 compensated linear vector  
 dipole (tension);  
 DC – double-couple;  
 NO – normal fault

**Fig. 4.** Location and moment tensor results for the tremor of  $M_L = 3.3$  on the mining map.

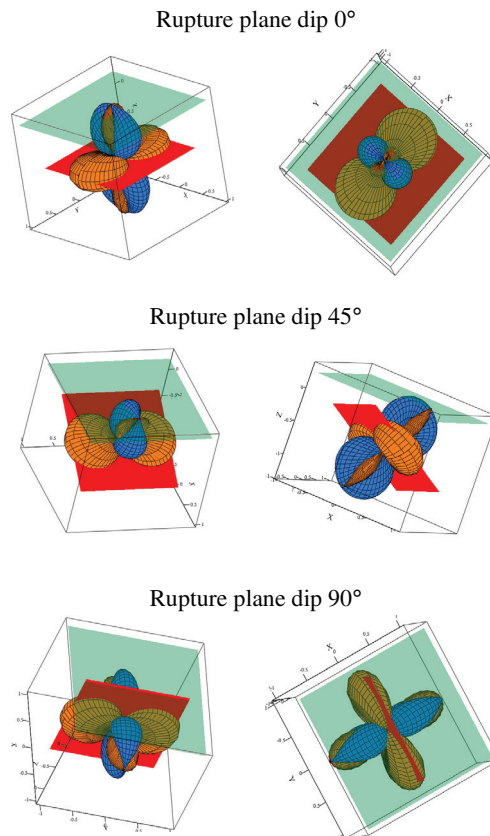


**Fig. 5.** Visualization of radiation pattern for SV- wave (blue) and SH-wave (yellow) for the rupture plane with dip of 0°, 45° and 90° (red) with respect to the horizontal plane (green) [20].



Long-term studies of seismic activity in USCB have shown [18, 19] that high energy tremors, the most dangerous for mining excavations, are characterized by shear slip, mathematically described by a double couple of forces. Radiations pattern for seismic waves propagation for the shearing mechanism can be graphically depicted [20]. With this type of focal mechanism are *S*-wave dominate. Figure 5 shows the spatial radiation pattern for the rupture planes with dip of 0°,45°and 90°with respect to the horizontal plane. *S*-wave radiation amplitudes image (waves with the highest amplitudes in the epicentral zone) was showing based on the parameters of the nodal plane A (strike 28°, dip 88°) of the tremor on June 21, 2016.This image along with the registered peak ground velocity values is shown in Figure 6a. The figure shows that the radiation pattern for *S*-wave emitted from the source of the tremor is not uniform, but there are privileged directions which confirm the registrations by more than half of the amplitude of ground vibrations at the S2 station compared to the ground vibrations recorded at the S1 station.

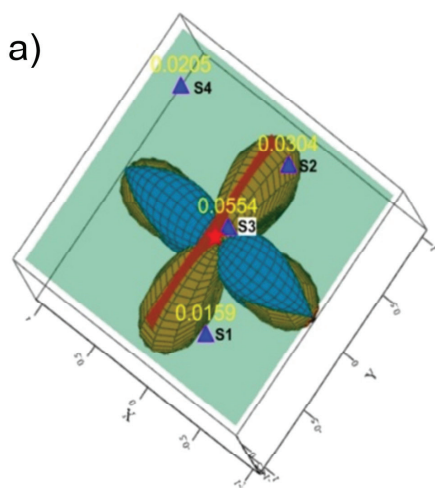


**Fig. 6a.** Radiation pattern for *S*-wave for the tremor registered on June 21, 2016 of magnitude  $M_L = 3.3$  for the focal mechanism shown in Figure 4.

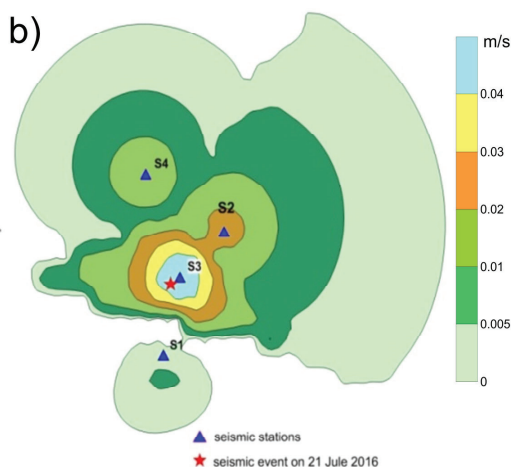


**Fig. 6b.** Distribution of differential velocity  $PGV_H^{dif}$  for tremor on June 21, 2016 of magnitude  $M_L = 3.3$ .

The theoretical distribution of the seismic radiation pattern for *S*-wave was compared with the “differential velocity amplitudes”  $PGV_H^{dif}$  for the tremor registered on June 21, 2016. The image of the “differential velocity amplitudes”  $PGV_H^{dif}$  is shown in Figure 6b. This image was obtained by subtracting the distribution of the vibration velocity amplitudes  $PGV_H^{amp}$  shown in Figure 3a from the distribution of the vibration velocity amplitudes  $PGV_H^{kor}(r_i)$  presented in Figure 3b. As presented, the distribution of “differential velocity amplitudes”  $PGV_H^{dif}$  in the epicentral zone is uneven and oriented according to the theoretical distribution radiation pattern for *S*-wave shown in Figure 6b. These calculations have shown that the highly probable factor affecting on the variation in measurement data ( $PGV_{Hp}$ ,  $PGA_{Hp10}$ ) at stations located almost at the same distance from the source area of the tremor may be the radiation pattern for *S*-wave, depending on the location of the rupture plane in the seismic event focus.

## 6 Conclusions

Analyzed case study of strong mining induced seismic event confirms that focal mechanism determining by a directional characteristics of the seismic radiation pattern has also impact on the distribution of horizontal peak ground velocity of vibration  $PGV_H$  on the surface.

The obtained results point out that in some cases of strong seismic events focal mechanism can distinctly change distribution of seismic parameters on the surface and consequently intensity of seismic influence.

The paper points out the necessity of elaboration a new empirical relationship with account of focal mechanism of the tremor and presents the developed methodology in this area.

It should be emphasized that solutions obtained in this area are not only cognitive but also practical, mainly due to the possibility of a more precise characteristic of mining activity impacting on environment.

## References

1. G. Mutke, J. Dworak, *Factors determining the effect of mining seismic events on buildings in the Upper Silesian Coal Basin. Selected issues of the geophysical studies in the mines – Lubiatów 1991*, Publ. Inst. Geophys. Pol. Acad. Sc. **M-16**, 245, 115-130 (in Polish) (1992)
2. Z. Zembaty A. Rutenberg, *Eng. Struct.* **24**, 11, 1485-1496 (2002) doi: 10.1016/S0141-0296(02)00096-2
3. D. Olszewska, S. Lasocki. *Application of the horizontal to vertical spectral ratio technique for estimating the site characteristics of ground motion caused by mining induced seismic events*. *Acta Geophysica Polonica*, **52**, 3, 301-318 (2004)
4. J.G. Anderson, *BSSA*. **100**, 1, 1-36. doi: 10.1785/0120080375 (2010)
5. S. Lasocki, *Acta Geophysica Polonica* **61**, 5, 1130-1155 (2013) doi:10.2478/s11600-013-0139-8
6. J. Chodacki, *Acta Geophysica Polonica* **64**, 6, 2449-2470 (2016) doi: 10.1515/acgeo-2016-0109
7. G. Mutke, K. Stec, *Seismicity in the Upper Silesian Coal Basin, Poland: Strong regional seismic events*. *Proc. 4th Int. Symp. - Rockbursts and Seismicity in Mines*, 213-217 (Rotterdam 1997)
8. A.F. Idziak, L. Teper, W.M. Zuberek, *Seismic activity and tectonics of the Upper Silesian Coal Basin Katowice*. *Publ. of Siles. Univ.* (in Polish) (1999)
9. H. Marcak, G. Mutke, *J. Seismol.* **17**, 4, 1139-1148, (2013) doi: 10.1007/s10950-013-9382-3
10. M. Kozłowska, B. Orlecka-Sikora, Ł. Rudziński, Sz. Cielesta G. Mutke, *Int. J. Rock Mech. Min.* **86**, 5-15 (2016) doi: 10.1007/s00024-016-1432-7
11. K. Stec, *Geophys. J. Int.* **168**, 2, 757-768 (2007) doi: 10.1111/j.1365-246X.2006.03227.x
12. G. Mutke, J. Dubiński. *Seismic intensity induced by mining in relations to weak earthquakes*. *Proc. of the 24th World Mining Congress. Part. Underground Mining*, 399-407 (Rio de Janeiro 2016)
13. E.F. Savarienskij, *Evaluation of the impact of near surface layer on the amplitude of ground motion*, *Izv. Akad. Nauk SSSR Geofizyka* **10**, 1441-1447 (in Russian) (1959)



14. G. Mutke, J. Chodacki, L. Muszynski, S. Kremers, R Fritschen, *Mining Seismic Instrumental Intensity Scale MSIS-15 – verification in coal basins*, AIMS 2015 - Fifth Int. Symp. Mineral Resources and Mine Development **14**, 551-560 (RWTH Aachen University 2015)
15. G. Mutke, H. Marcak, F. Mutke, A. Barański, *The method of determining the distribution maps of seismic intensity IGSI after recording of a strong seismic event induced by mining*, Przegląd Górniczy, **2**. 51-58 (in Polish) (2017)
16. G. Kwiatek, P. Martínez-Garzón, M. Bohnhoff, *Seismol. Res. Lett.*, **87**, 4 (2016) doi:10.1785/0220150251
17. K. Aki, P.G. Richards, *Quantitative Seismology – Theory and Methods* (W. H. Frejman & Co., San Francisco 1980)
18. K. Stec, *Arch. Min. Sci.* **57** 4, 871–886 (2012) doi: 10.2478/v10267-012-0057-7
19. K. Stec, *Journal of Sustainable Mining*, **1/2015**, 55-65 (2015) doi: 10.1016/j.jsm.2015.08.008
20. A. Lurka, *Kierunkowość radiacji sejsmicznej (Directionality of the seismic radiation pattern)* in: *Geologiczne przyczyny wzmacniania drgań w nadkładzie serii węglowej na obszarze Górnośląskiego Zagłębia Węglowego* (ed. K. Stec), 43-46 (in Polish) (CMI, Katowice, 2013)